

p-Nitronaphthylaniline in the presence of *N,N*-dimethylaniline as bimolecular photoinitiating system of polymerization

A. Costela^a, I. García-Moreno^{a,*}, O. García^b, R. Sastre^b

^a Instituto Química-Física 'Rocasolano', C.S.I.C., Serrano 119, 28006 Madrid, Spain

^b Instituto de Ciencia y Tecnología de Polímeros, C.S.I.C., Juan de la Cierva 3, 28006 Madrid, Spain

Received 22 November 1999; accepted 26 November 1999

Abstract

Photophysics, photochemical and polymerization activity of *p*-nitronaphthylaniline (NNA) in the presence of *N,N*-dimethylaniline (DMA) as coinitiator was analyzed to establish the influence of the initiator nature on the photosensitized generation of free radicals derived from DMA. Steady-state (365 nm) photolysis was carried out and detailed studies of the spectroscopy of both reactants were accomplished. The coinitiator DMA induces the photoreduction of NNA with a very low photoreduction quantum yield, although the stoichiometry of the reaction revealed that up to 570 molecules of DMA are consumed by each NNA molecule photoreduced. The efficiency of NNA/DMA system as photoinitiator was studied following the polymerization kinetics of lauryl acrylate monomer by Differential Scanning Photo-Calorimetry. The photosensitization of DMA through the excitation energy transfer of NNA, working concurrently to the photoreduction reaction, induces a high polymerization efficiency with a very low consumption of the initiator in a catalyzer-like way. ©2000 Elsevier Science S.A. All rights reserved.

Keywords: *p*-Nitronaphthylaniline (NNA); *N,N*-dimethylaniline (DMA); *p*-Nitroaniline (*p*NA); Photoinitiator; Photochemical; Polymerization; Photolysis

1. Introduction

Industrial use of photopolymerization reactions demands the development of more effective photoinitiators [1–9], a key component in light-induced radical polymerization since, through a photochemical reaction, they produce efficiently free radicals which attach themselves to the double bond of the polymerizable component(s).

Increased requests for improved photoinitiators motivated our recent investigations on the photochemistry and polymerization activity of a new bimolecular photoinitiator system, based on *p*-nitroaniline (*p*NA) with a tertiary amine (DMA) acting as reductor agent [10–13]. The photoreduction process involves an electron–proton transfer from the ground state of the tertiary amine to the lowest excited triplet state of the initiator, generated with high yield by UV irradiation, leading to 1,4-benzenediamine, as the main photoreduction product, and to α -alkylamino radicals from the tertiary amine, which are the actual initiating species of polymerization in the present system.

Although, DMA induced the photoreduction of *p*NA with a very low quantum yield, this initiator exhibits an

unexpected high polymerization efficiency, higher than that of well-known photoinitiators of industrial importance (i.e. aromatic ketones), suggesting a new, more efficient mechanism of bimolecular photoinitiation [14]. The *p*NA initiator sensitizes the generation of α -alkylamino radicals derived from DMA coinitiator through an excitation energy transfer, inducing the homolytic scission of its weakest molecular bond, yielding an avalanche of reactive species without consuming *p*NA, which acts as a mere photosensitizer of the triplet state of the tertiary amine in a catalyzer-like way [14]. To the best of our knowledge, the *p*NA–DMA system was the first bimolecular photoinitiator based on this mechanism which overturns the well-established behavior on which the development of bimolecular photoinitiators has been based up to now.

In the conventional approach, the generation of free radicals takes place through a stoichiometric photoreduction of the initiator induced, with a high quantum yield, by the coinitiator. Depending on the type of initiator–coinitiator pair, this reaction basically proceeds through direct hydrogen abstraction or electron–proton transfer, although under certain conditions both mechanisms may be competitively involved. In any case, the reaction occurs from the triplet state of the initiator, formed with high yield under UV irradiation, and

* Corresponding author.

characterized by a long lifetime, of the order of hundred of microseconds in solution at room temperature, which determines that the bimolecular photoreduction can compete efficiently with any other radiative or radiationless decay channels. In the new initiation mechanism, the triplet state of the initiator has to be a short-lived intermediate (of the order of a few nanoseconds or less), in order to increase the efficiency of the excitation energy transfer against other bimolecular deactivation reactions. Likewise, the coinitiator molecule has to contain a bond with a dissociation energy lower than that of this triplet excited state, to induce its homolytic scission with formation of reactive initiating species.

The actual possibilities of this new and promising mechanism of photosensitized polymerization encouraged us to extend the investigation to different *p*NA derivatives in order to establish the energetic, photophysical and structural requirements of new and more efficient initiators. The present paper is devoted to explore the potential of *p*-nitronaphthylaniline (NNA) in the presence of DMA as bimolecular photoinitiator. To this purpose, its photophysical and photochemical behavior was analyzed under steady-state condition. The spectral and temporal characteristics of the lowest excited states of the reactants are studied by time-resolved spectroscopy. The stoichiometry and mechanism of the photoreduction reaction was analyzed following the consumption rate of both reactants as a function of the irradiation time under aerobic and steady-state photolysis conditions at 365 nm. In addition, the photopolymerization activity of NNA/DMA system was studied following by differential scanning photocalorimetry (Photo-DSC) the kinetic of the photoinduced polymerization of lauryl acrylate (LA). The results of this study provide valuable information to understand the basis and fundamentals of the new photoinitiation mechanism of radical polymerization.

2. Experimental

2.1. Materials

Ethyl acetate (AcOEt) (Sigma-Aldrich, HPLC grade) was dried over molecular sieves with pore diameter of 4 Å. NNA and *p*NA (Aldrich, 99% purity) were recrystallized from ethanol and water, respectively. Lauryl acrylate (Pluka Chemie, Tech.) was distilled under reduced pressure prior to use and DMA (Carlo Erba) was dried over potassium hydroxide, distilled under reduced pressure and stored under nitrogen atmosphere in the dark at low temperature.

2.2. Steady-state photolysis

The irradiation system and the experimental procedure employed have been described previously [10]. Briefly,

the irradiation wavelength of 365 nm was selected from a Philips high pressure mercury lamp (Hg-CS 500/2) with a Kratos monochromator (model CM 252). The absorbed light intensity at the irradiation wavelength was measured using an International Light Digital Radiometer (model 11700). Aberchrome 540 actinometer [15] was used to calibrate the digital display of the radiometer to an absolute value for the number of quanta incident per unit of time. The photolysis of the sample was monitored by measuring the change in the maximum of the UV absorption curve.

2.3. Photocalorimetry

The kinetics of the photoinitiated polymerization was monitored using a Photo-DSC system [16]. NNA was dissolved in pure LA at a concentration of $\approx 5 \times 10^{-3}$ M ensuring total absorption of the 365 nm radiation in the 0.12 cm of path-length. The incident light intensity was kept constant at a value of 1.9×10^4 einstein $l^{-1} s^{-1}$. DMA was added as a coinitiator at concentrations ranging from 10^{-2} to 1.5×10^{-1} M. Prior to irradiation, the sample of 20 μ l was equilibrated to the operating temperature of 40°C for 15 min. Then, the samples were irradiated for up to 20 min under aerobic and anaerobic conditions. In the kinetics study care was taken to maintain the conversions lower than 25%, since under these conditions the relationship between conversion of the monomer and irradiation time remains linear. A more detailed description of the general procedure followed and the determination of incident light intensity can be found elsewhere [16,17].

2.4. Measurement of the consumption rate of NNA and DMA

The consumption rate of both components of this photoinitiating system was followed as a function of the irradiation time under steady-state photolysis conditions at 365 nm. The volume of the irradiated mixture in the quartz cell was 3.5 ml. At different irradiation times, aliquots of 25 μ l were drawn from the medium to follow the evolution of DMA while the rest of the mixture was analyzed spectrophotometrically to follow the photoreduction of NNA measuring the decrease of its absorbance at the maximum wavelength (406 nm). The consumption of DMA was monitored by high performance liquid chromatography (HPLC) (Waters M-45 HPLC pump, Spectra Physics 100 ultraviolet detector). The stationary phase was Spherisorb ODS-2-C₁₈, 5 μ m (Trace Analytica) (125 mm \times 4 mm ID). The eluent was 7/3: Methanol/Water (v/v)+1 vol % of triethanolamine solution. The flow rate was 1 ml min^{-1} and the detector was set at 300 nm. DMA standards of 0.1–10 mM were run for a calibration curve. Under this conditions, the DMA retention time was 2.1 ± 0.1 min.

2.5. Spectroscopic measurements

The UV absorption spectra of the samples were recorded at room temperature with both Perkin–Elmer Lambda 16 and Shimadzu UV-265F5 spectrophotometers. Emission spectra from the samples were recorded on a Perkin–Elmer LS-SOB luminiscence spectrometer. Quantum yields of fluorescence (ϕ_F) were determined at room temperature by comparison with 9,10-diphenylanthracene as standard and assuming a value of 1 in cyclohexane [18]. Quantum yields of phosphorescence (ϕ_P) were obtained at 77 K by comparison with benzophenone as standard and assuming a value of 0.74 in ethanol [19].

3. Results and discussion

3.1. Spectroscopic characteristics

The absorption spectrum of NNA in a 10^{-4} M ethyl acetate solution is shown in Fig. 1. The absorption maximum observed around 406 nm corresponds to a $n-\pi^*$ band [22] and is red-shifted with respect to the absorption spectrum of *p*NA (~ 50 nm) [10]. This pronounced bathochromic shift is a consequence of the increased electron density of the anilino nitrogen caused by electron-donating effect of the aromatic group. The molar absorption coefficient of NNA in ethyl acetate solution at 406 nm is $16707 \text{ M}^{-1} \text{ cm}^{-1}$. The presence of a tertiary amine in the solution does not induce significant variations in the absorption characteristics of the initiator.

This nitronaphthyl derivative fluoresces very weakly ($\phi_F=10^{-5}$), with an emission centered at 462 nm (see Fig. 1), and exhibits a phosphorescence emission ($\phi_P=3 \times 10^{-4}$),

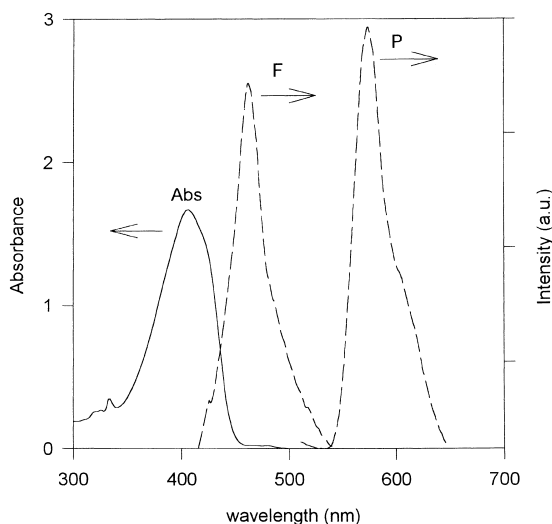


Fig. 1. Absorption (Abs), fluorescence (F) and phosphorescence (P) spectra (at 77 K) of a 10^{-4} M ethyl acetate solution of NNA. Excitation wavelength: 406 nm.

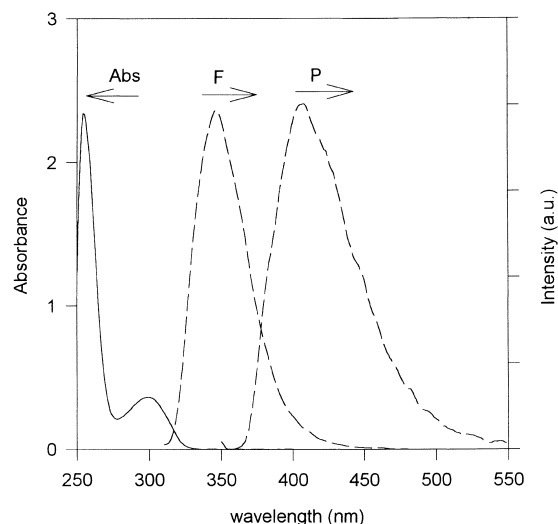


Fig. 2. Absorption (Abs), fluorescence (F) and phosphorescence (P) spectra (at 77 K) of a 10^{-4} M ethyl acetate solution of DMA. Excitation wavelength: 300 nm.

direct indication of a significant intersystem crossing between the S_1 and T_n excited states of the molecule [20]. The phosphorescence spectrum of a 10^{-4} M ethyl acetate solution of NNA, registered at 77 K, is also shown in Fig. 1. The excitation wavelength was 406 nm and the delay time between excitation and detection 0.1 ms. Phosphorescence emission is centered at 572 nm with a triplet lifetime of 36 ms, much shorter than the $\pi\pi^*$ triplet state of *p*NA (300 ms), revealing the $n\pi^*$ character of the lowest triplet state of NNA molecule [20]. The absorption spectrum of DMA in a 10^{-4} M ethyl acetate solution is shown in Fig. 2, together to its emission spectra induced by excitation at 300 nm and registered under the above described experimental conditions. By contrast to the initiator NNA, the coinitiator DMA exhibits strong emissions of fluorescence ($\phi_F=1.5 \times 10^{-2}$), centered at 345 nm, and phosphorescence ($\phi_P=0.3$), centered at 411 nm. The increasing aromaticity of NNA with respect to *p*NA leads to a significant decrease of the energy resonances between the excited states of NNA and DMA that could result in a reduction on the photosensitization efficiency of DMA through the excitation energy transfer from NNA molecule.

3.2. Steady-state photolysis of NNA

Steady-state photolysis of NNA and its consumption rate, R_{NNA} , were studied by irradiating at 365 nm under anaerobic conditions and constant incident light intensity, $I_0=5.1 \times 10^{-6} \text{ einstein l}^{-1} \text{ s}^{-1}$, a 10^{-4} M ethyl acetate solution of this initiator. Quantum yields of chromophore disappearance, ϕ_{NNA} , were determined by UV–Vis spectroscopy following the decrease in the maximum of the initiator absorption band (406 nm) with irradiation time as has been reported previously [21]. The steady-state photolysis of NNA

is characterized by a low quantum yield, $\phi_{\text{NNA}}=2.2\times 10^{-3}$, reflecting its stability under UV irradiation. This quantum yield is higher than that determined for *p*NA under identical experimental conditions, $\phi_{\text{NNA}}=1.4\times 10^{-3}$.

As was seen for *p*NA, the presence of oxygen does not induce a significant variation on the quantum yield of NNA disappearance ($\phi_{\text{NNA}}=1.9\times 10^{-3}$).

The disappearance of NNA induced by irradiation under the above described experimental conditions, exhibits a linear dependence on the irradiation time, with its slope of $1.1\times 10^{-8}\text{ M s}^{-1}$, being the consumption rate of NNA, R_{NNA} . Following the same behavior to that exhibited by the photolysis quantum yield, the consumption rate of NNA is slightly higher than that of *p*NA determined under identical experimental conditions, $R_{\text{pNA}}=6.8\times 10^{-9}\text{ M s}^{-1}$, and this kinetic parameter does not show a significant dependence on the presence of oxygen ($R_{\text{NNA}}=8.8\times 10^{-9}\text{ M s}^{-1}$), direct consequence of a photolysis reaction that occurs from a very short-lived triplet state.

3.3. Photoreduction process of NNA

The photoreduction process of NNA induced by DMA followed by UV–Vis spectroscopy was analyzed for different amounts of DMA added to a constant concentration (10^{-4} M) of NNA. The following NNA/DMA molar ratios were used: 1/2, 1/5, 1/10 and 1/20. Fig. 3 shows the dependence on the irradiation time of the absorption spectrum for an ethyl acetate solution of NNA/DMA in a molar ratio 1/10 irradiated at 365 nm under anaerobic and steady-state conditions. The chromophore disappearance, revealed by the

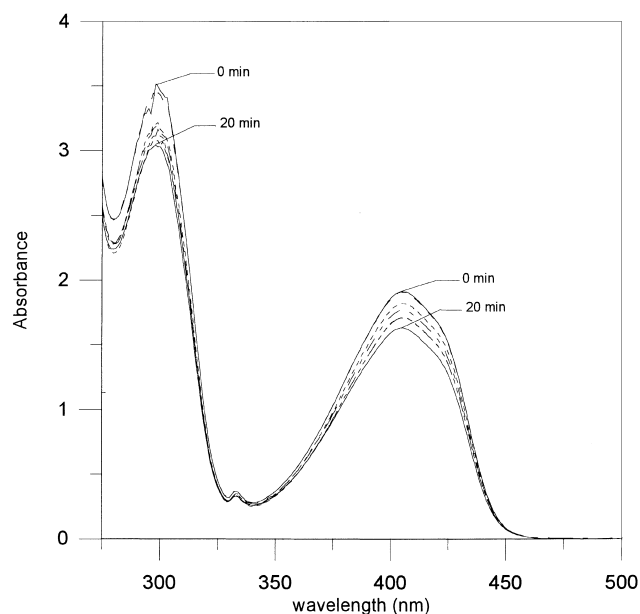


Fig. 3. Dependence of the UV–Vis absorption spectrum of a 10^{-4} M ethyl acetate solution of NNA with a molar ratio of DMA 1/10 on the irradiation time under steady-state conditions in an anaerobic atmosphere. Irradiation wavelength: 365 nm.

decrease in its absorption maximum, is accompanied by a decrease of the absorption intensity at shorter wavelengths assigned to the tertiary amine. The irradiation of the sample for a long time does not modified the spectroscopic features aforementioned which is a prior indication of a photoreduction process slower and less efficient than that induced for DMA in the presence of *p*NA [11].

The photoreduction quantum yield of NNA induced by DMA, ϕ_{NNA} , under different experimental conditions, are summarized in Table 1. For comparison, the data determined in the photoreduction of *p*NA induced by DMA under identical experimental conditions are also included in this table. Following the same behavior to that exhibited by the *p*NA/DMA system, the presence of DMA as coinitiator induces only a slight increase in ϕ_{NNA} with respect to that determined in the photolysis process. The efficiency of DMA inducing the photoreduction of NNA is much lower than that exhibited by *p*NA. The higher stability of this nitro-compound towards its photoreduction by tertiary amines could be related to both a higher charge-transfer character of the lowest excited state [22] and a faster competing radiationless deactivation processes, resulting in a shorter lifetime of its lowest triplet state.

On the other hand, ϕ_{NNA} is critically dependent on the presence of oxygen. Thus, under anaerobic conditions, the photoreduction quantum yield increases up to a factor of 2 reaching a value of 4.2×10^{-3} . As discussed in a previous work [11], the lower efficiency of the photoreduction process under aerobic conditions could be ascribed to photooxidation reactions of the α -aminoalkyl radicals derived from the tertiary amine [23,24].

The consumption rate of NNA and DMA, R_{NNA} and R_{DMA} , respectively, were also analyzed from a 10^{-4} M ethyl acetate solution of NNA with different molar ratios to DMA irradiated, under aerobic conditions, at 365 nm with an incident light intensity $I_0=1.4\times 10^{-6}\text{ einstein l}^{-1}\text{ s}^{-1}$. The values obtained for these kinetic parameters are summarized in Table 1 together to those evaluated for the *p*NA/DMA system.

Fig. 4 shows the dependence of the consumption of both reactants on the irradiation time. The DMA disappearance increases linear and drastically with the irradiation time until a degree of conversion near 30% is reached. Further increase of the irradiation time beyond this point does not modify significantly the consumption rate of the tertiary amine. The parameter R_{DMA} is deduced from the slope of the line fitted to these experimental data within the time interval where it exhibits a linear behavior. This disappearance rate is much higher than that of the NNA photoinitiator, for all NNA/DMA molar ratios selected. In addition, R_{DMA} increases with the tertiary amine concentration following a linear relationship. However, as is reported in Table 1, the parameter R_{DMA} induced by NNA is much lower than that determined by *p*NA. This fact could be ascribed to a worst overlap between the energy levels of NNA and DMA reducing the effectiveness of the excitation energy transfer and,

Table 1

Influence of the molar ratio of DMA, $[DMA]_r$, added to NNA on its photoreduction quantum yield, ϕ_{NNA} , and on the consumption rate of both reactants, R_{NNA} and R_{DMA} , under aerobic conditions. For comparison, the values of the kinetic parameters obtained for the pNA/DMA system under identical experimental conditions are included^a

$[DMA]_r$	NNA/DMA			pNA/DMA		
	$10^3 \times \phi_{NNA}$	$10^8 \times R_{NNA}$ ($M s^{-1}$)	$10^8 \times R_{DMA}$ ($M s^{-1}$)	$10^3 \times \phi_{pNA}$	$10^8 \times R_{pNA}$ ($M s^{-1}$)	$10^8 \times R_{DMA}$ ($M s^{-1}$)
1/0	1.9	0.9		1.3	0.6	
1/2	2.0	0.3	7.9	13.2	1.7	51.3
1/5	2.3	0.3	51.4	13.2	1.7	138.2
1/10	2.3	0.3	76.8	13.2	1.7	148.5
1/20	2.5	0.3	187.9	13.2	1.7	195.4

^a Experimental conditions: photoinitiator concentrations, 10^{-4} M; irradiation wavelength, $\lambda_{irr}=365$ nm; incident light intensity, $I_0=1.4 \times 10^{-6}$ einstein $l^{-1} s^{-1}$.

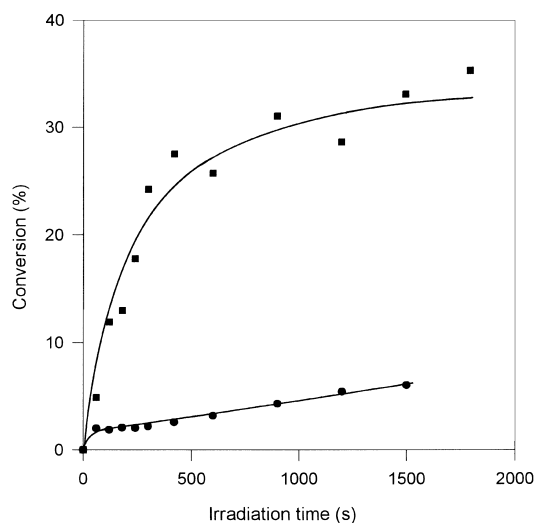


Fig. 4. Dependence of the degree of conversion of NNA (●) and DMA (■) on the steady-state irradiation time at 365 nm of a 10^{-4} M ethyl acetate solution of NNA/DMA 1/10 molar ratio under aerobic conditions. The solid lines represent an eyeball fit to the data points.

consequently, it would be expected a lower activity in the initiation process of polymerization with respect to that reached by the pNA/DMA system. In the presence of oxygen, the photooxidation of the tertiary amine leads to an increase of R_{DMA} by a factor of 2.

The stoichiometry of the reaction, evaluated from the ratio of the slopes of the lines fitted to the both reactants consumption, indicates that up to 570 molecules of DMA are consumed per each NNA molecule photoreduced. Taking into account the low photoreduction quantum yield of NNA promoted by DMA, the rapid consumption of the coinitiator confirms that the photoreduction process is competing with a photosensitization process of DMA, through an excitation energy transfer from NNA, yielding an avalanche of α -alkylamino radicals, without the consumption of the initiator, following the same effective mechanism described in detail for the pNA/DMA photoreaction [14]. Experimental evidence of this photosensitization process is provided by the emission properties of an ethyl acetate solution of NNA with and without DMA (Fig. 5). Irradiation at 406 nm of pure

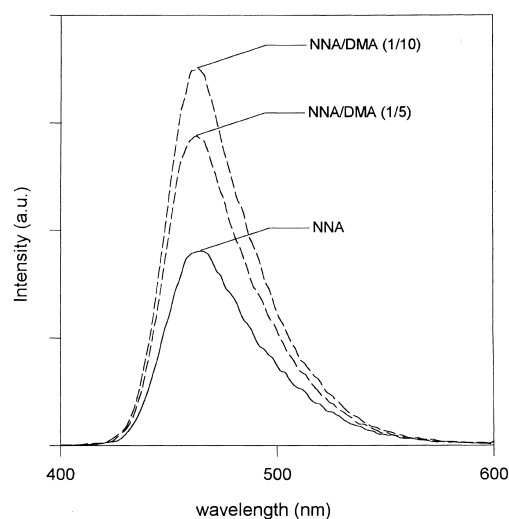


Fig. 5. Emission spectra of an ethyl acetate solution of NNA with and without DMA after irradiation at 406 nm. The increasing (NNA/DMA) molar proportions are indicated in parenthesis.

NNA induces a weak emission centered at 462 nm, assigned to the fluorescence band of this molecule. The presence of DMA, which does not absorb at the irradiation wavelength, modifies significantly the recorded emission which experiences a clear increase in intensity. Taking into account that the DMA molecule emits phosphorescence in the same spectral region where fluorescence of NNA appears with a quantum yield 4 orders of magnitude higher than ϕ_F of NNA, the behavior of the emission of the NNA solution in the presence of increasing amounts of DMA is consistent with phosphorescence of DMA being emitted concurrently with fluorescence of NNA. A more direct experimental evidence of the proposed process would require a time-resolved analysis in the sub-nanosecond time domain due to the very short lifetimes involved.

3.4. Photoinitiation of polymerization

Different experiences have revealed that NNA or DMA alone are incapable of initiating efficiently the polymerization of LA even over extensive periods of time at 40°C

in the dark or under illumination. When used in combination, however, they readily initiate LA polymerization but only under irradiation. This photoinitiated polymerization was found to be inhibited by hydroquinone, confirming that the process takes place by a radical mechanism. As was previously discussed for the *p*NA–DMA system, the radicals derived from the tertiary amine are the main and most active species in the initiation mechanism [12]. The kinetic of photoinitiation of LA was monitored by Photo-DSC. Exotherm rates as a function of time were observed under isothermal conditions for continuous illumination reactions. Initial rates of polymerization R_p were calculated from the slopes of the plots of polymerized monomer concentration versus irradiation time, in the time interval where this conversion change exhibits a linear behavior. Polymerization quantum yields (ϕ_m) were determined from the slope of the line best fitting the experimental linear dependence found when the amount of monomer polymerized is represented as a function of the absorbed light intensity, I_a .

The influence of both the DMA concentration and the nature of the photoinitiator on the polymerization process is reflected in Table 2, where the values obtained for the kinetic parameters in the bulk polymerization of LA induced by both NNA and *p*NA under identical experimental conditions are reported. Under anaerobic conditions, R_p and ϕ_m increases with the amine concentration, although the relationship is not linear since above the 1/10 NNA/DMA molar ratio both polymerization parameters become much less dependent on the DMA concentration. NNA derivative is more efficient in the polymerization process than in the photoreduction reaction, a direct consequence to the generation up to 570 α -alkylamino radicals from DMA for each NNA molecule photoreduced.

Under aerobic conditions, the kinetic parameters of photopolymerization are, at least, three times lower than in nitrogen atmosphere (see Table 2). This effect reveals the role of the molecular oxygen as inhibitor of radical-induced polymerization because of its high reactivity toward radical species.

Table 2

Rate (R_p) and quantum yield (ϕ_m) of polymerization of LA photoinduced by both initiators, NNA and *p*NA, in the presence of different molar ratios of DMA as coinitiator, $[DMA]_r$, under aerobic and anaerobic conditions^a

$[DMA]_r$	NNA/DMA				<i>p</i> NA/DMA			
	$10^3 \times R_p$ ($M s^{-1}$)		ϕ_m		$10^3 \times R_p$ ($M s^{-1}$)		ϕ_m	
	N ₂	O ₂	N ₂	O ₂	N ₂	O ₂	N ₂	O ₂
1/2	5.7	1	29.9	5.2	4.9	0.6	26.0	3.1
1/5	6.3	0.9	33.0	4.6	5.7	0.7	30.2	3.7
1/10	8.8	1.5	46.3	8.1	12.6	0.7	66.9	3.9
1/20	9.7	1.6	51.1	7.9	19.4	3.2	103.0	16.9
1/30	9.7	3.6	51.2	18.9	20.6	3.8	108.7	19.8

^a The selected concentrations of initiators, $[pNA]=2.1 \times 10^{-3}$ M and $[NNA]=5.2 \times 10^{-3}$ M, assure identical absorbed light intensity at 365 nm, $[Abs=2]$.

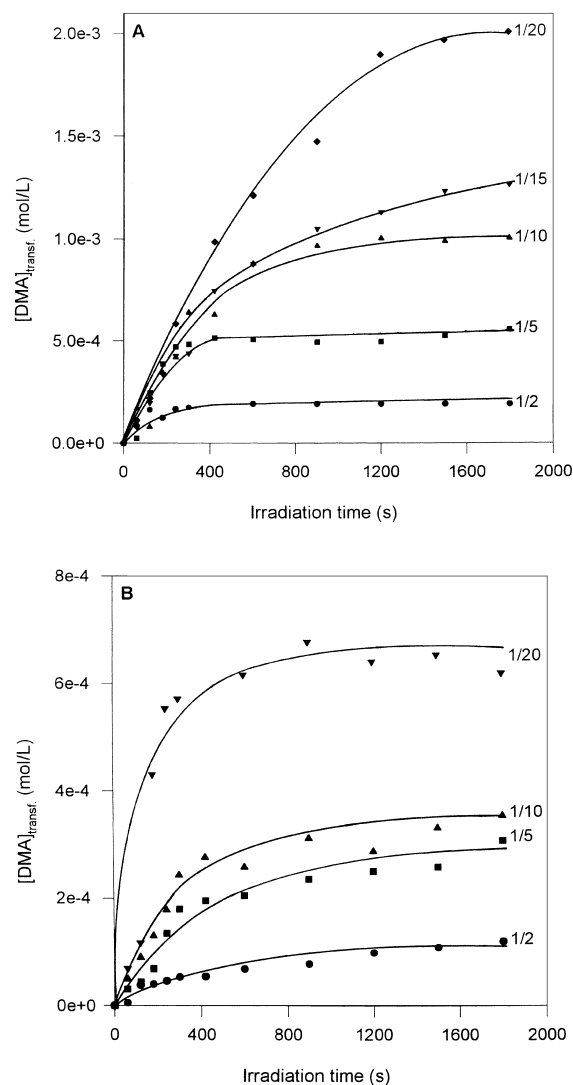


Fig. 6. Dependence of the concentration of DMA consumed on the steady-state irradiation time at 365 nm under aerobic conditions of a 10^{-4} M ethyl acetate solution of *p*NA(A) and NNA (B) with different molar proportions of DMA.

The kinetic parameter induced by NNA and *p*NA follow the same dependence on DMA concentration, although, for initiator/DMA molar ratios higher than 1/10, the higher aromaticity of NNA with respect to *p*NA initiator results in a remarked decrease of its polymerization activity, in good agreement with the consumption rates of NNA and DMA much lower than those induced by *p*NA/DMA system. However, under both aerobic and anaerobic conditions, the presence of low amine concentration reverses the above behavior with NNA inducing R_p and ϕ_m slightly higher than those exhibited by *p*NA in spite of its lower DMA consumption rate. This behavior could be reflecting the influence on the photopolymerization of the global kinetics followed for the generation of the initiating free radicals during the total irradiation time. Under certain experimental conditions, this kinetics could not be properly related to R_{DMA} , since

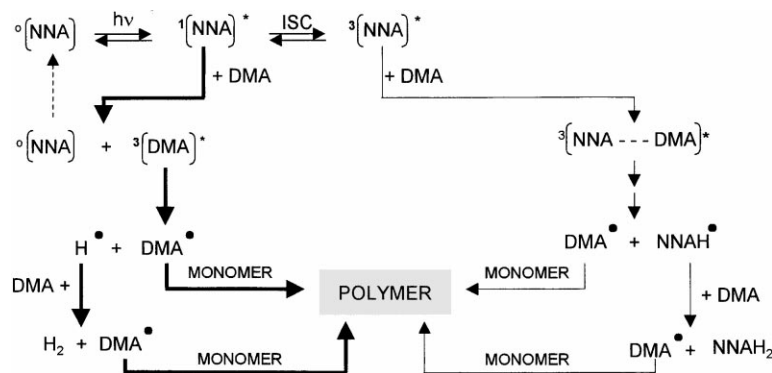


Fig. 7. Mechanism for the photoreaction of NNA in the presence of DMA under UV irradiation. The photoreduction process (right) is a minor pathway as compared with the efficient photosensitization of DMA by NNA (left) leading to an enhanced polymerization activity in spite of a very low photoreduction quantum yield.

this parameter was deduced within the time domain where DMA consumption followed a linear behavior. Fig. 6 shows the dependence of the coinitiator conversion on the irradiation time induced by both initiators, *p*NA and NNA, in the presence of increasing amounts of DMA. At the lowest amine concentration, NNA derivative induces a consumption of DMA slower but more continued along the irradiation time of polymerization (1200 s) than that determined by *p*NA where DMA is totally consumed in the first 400 s of irradiation. Under these experimental conditions, the high and almost instantaneous concentration of initiating radicals could enhance the probability of secondary reactions (re-combinations, reactions between free radicals and macroradicals, etc.) able to compete with the own polymerization reducing significantly the rate and efficiency of this process. However, as the DMA proportion increases into the sample, its conversion degree becomes more progressive resembled the behavior induced by NNA. These are the samples where an apparent direct relationship between R_{DMA} and the kinetic parameters R_p and ϕ_m can be established — the higher consumption of DMA, the higher rate and efficiency of polymerization.

According to the conclusions extracted from the *p*NA/DMA photoinitiating system and the present study and taking into account the spectroscopic characteristics of both reactants, NNA and DMA, our findings strongly suggest the pathways indicated in Fig. 7 as the most probable mechanism for the photoreaction of NNA in the presence of DMA under UV irradiation. The photosensitization process of the triplet state of DMA by NNA is reflected in an enhanced of the polymerization efficiency with respect to other conventional photoinitiators [11]. Moreover and taking into account that the initiator is the active specie in the absorption of the irradiation light, the low consumption of NNA is assuring the same efficiency of the primary step of this initiating mechanism along the monomer polymerization. Consequently, higher initiation efficiency achieved with a reduced consumption of the initiator represents an important economical advantage from an industrial point of view.

Acknowledgements

This work was supported by Projects MAT97-0705-C02-01 and MAT97-0727 of Spanish Comision Interministerial de Ciencia y Tecnologia.

References

- [1] F. Brickman, G. Delzenne, A. Poot, J. Willems, *Unconventional Imaging Processes*, Focal Press, London, 1977.
- [2] S.P. Pappas, *UV Curing: Science and Technology*, vol. 1, Stanford Technology Marketing Corporation, USA, 1978; and *ibid.*, vol. 2, 1982.
- [3] C.G. Roffey, *Photopolymerization of Surface Coatings*, Wiley/Interscience, Chichester, UK, 1982.
- [4] R. Phillips, *Sources and Applications of Ultraviolet Radiation*, Academic Press, New York, 1983.
- [5] J.F. Rabek, *Mechanisms of Photophysical Processes and Photochemical Reaction in Polymers*, Wiley, New York, 1987.
- [6] J.P. Fouassier, in: J.F. Rabek (Ed.), *Photochemistry and Photophysics*, vol. 2, CRC Press, Boca Raton, FL, 1990, (Chapter 1).
- [7] E.A. Lissi, M.V. Encinas, in: J.F. Rabek (Ed.), *Photochemistry and Photophysics*, vol. 4, CRC Press, Boca Raton, FL, 1991, (Chapter 4).
- [8] K.K. Dietliker, in: P.K.T. Oldring (Ed.), *Chemistry and Technology of UV and EB Formulations for Coating, Inks and Paints*, vol. 3, Sita Technology, London, 1991.
- [9] J.P. Fouassier, J.F. Rabek (Eds.), *Radiation Curing in Polymer Science and Technology*, vol. 4, Elsevier, London, 1993.
- [10] A. Costela, I. Garcia-Moreno, J. Dabrio, R. Sastre, J. *Photochem. Photobiol. A: Chem.* 109 (1997) 77.
- [11] A. Costela, I. Garcia-Moreno, J. Dabrio, R. Sastre, J. *Polym. Sci.: Part A: Polym. Chem.* 35 (1997) 3801.
- [12] A. Costela, I. Garcia-Moreno, J. Dabrio, R. Sastre, *Macromol. Chem. Phys.* 198 (1997) 3787.
- [13] A. Costela, I. Garcia-Moreno, J. Dabrio, R. Sastre, *Acta Polymerica* 48 (1997) 423.
- [14] A. Costela, I. Garcia-Moreno, O. Garcia, R. Sastre, *Chem. Phys. Lett.* (1999), submitted for publication.
- [15] H.G. Heller, J.R. Langan, *J. Chem. Soc. Perkin Trans. 2* (1981) 341.
- [16] R. Sastre, M. Conde, F. Catalina, J.L. Mateo, *Rev. Plas. Mod.* 393 (1989) 375.
- [17] J.L. Mateo, P. Bosch, F. Catalina, R. Sastre, *J. Polym. Sci. Polym. Chem. Ed.* 30 (1992) 829.
- [18] J.C. Scaiano, *Handbook of Organic Photochemistry*, vol. 1, CRC Press, Boca Raton, FL, 1989, (Chapter 16).

- [19] J.N. Demas, G.A. Grosby, *J. Phys. Chem.* 75 (1971) 91.
- [20] J. Malkin, *Photophysical and Photochemical Properties of Aromatic Compounds*, CRC Press, Boca Raton, FL, 1992, (Chapter 14).
- [21] J.L. Mateo, J.A. Manzarbeitia, R. Sastre, *J. Photochem. Photobiol. A: Chem.* 40 (1987) 169.
- [22] D. Döpp, *Top. Curr. Chem.* 55 (1975) 49.
- [23] R.F. Bartholomew, R.S. Davidson, *J. Chem. Soc. C* 2342 (1971).
- [24] R.S. Davidson, in: J.P. Fouassier, J.F. Rabek (Eds.), *Radiation Curing in Polymer Science and Technology*, vol. 3, Elsevier, Barking, 1993, pp. 153–176.